# MULTI-FREQUENCY SAR CAPABILITIES FOR FOREST BIOMASS AND CARBON INVENTORY FOR REDD MONITORING

Suman Sinha[1*], A. Santra[2], S. S. Mitra[3], C. Jeganathan[4], L. K. Sharma[5], M. S. Nathawat[6], A. K. Das[7] and S. Mohan[8]

[1]Haldia Institute of Technology, Haldia 725657, India,
Email: sumanrumpa.sinha@gmail.com
[2]Haldia Institute of Technology, Haldia 725657, India,
Email: avisek.santra@gmail.com
[3]Haldia Institute of Technology, Haldia 725657, India,
Email: shreyashi.mitra@gmail.com
[4]Birla Institute of Technology, Mesra 835215, India,
Email: jeganathanc@bitmesra.ac.in
[5]Central University of Rajasthan, Ajmer 305817, India,
Email: laxmikant1000@yahoo.com
[6]Indira Gandhi National Open University, New Delhi 110068, India,
Email: msnathawat@ignou.ac.in
[7]Space Application Centre (ISRO), Ahmedabad 380015, India,
Email: anup@sac.isro.gov.in
[8]Physical Research Laboratory, Ahmedabad, 380059, India,
Email: shivmohan.isro@gmail.com

**KEY WORDS :** ALOS PALSAR, Radarsat-2, COSMO-Skymed, Forest, Biomass.

**ABSTRACT :** Greenhouse gas inventories and emissions reduction programs require robust methods to quantify carbon sequestration in forests. Proper inventory of forest aboveground biomass (AGB) is required for accounting carbon emissions that forms the most vital part of the carbon cycle modeling and climate change mitigation programs in context to Reducing Emissions from Deforestation and Forest Degradation (REDD). Remote Sensing (RS) technology provides cost and time effective means for accurate temporal monitoring over large synoptic extents at local to global levels, and hence, is beneficial over conventional methods. The study presents a suitable approach for estimating AGB through the synergic use of multi-frequency X-, C- and L-band Synthetic Aperture Radar (SAR) data over tropical deciduous mixed forests of Munger (Bihar, India). Backscatter values generated from the raw SAR images were correlated with field-based AGB values and then regressed to generate best-fit models for AGB estimates with single and combined frequencies of COSMO-Skymed (X-band), Radarsat-2 (C-band) and ALOS PALSAR (L-band). Among all the models for AGB estimation, the integrated model involving X, C- and L-bands showed the best results with $r^2$=0.95, RMSE=14.81 t/ha and Willmott's index of agreement of 0.95. Resulting modeled AGB were converted to carbon (C) and carbon dioxide ($CO_2$) equivalents using conversion factors. Hence, the study proposed L-band for single frequency analysis and the combination of X-, C- and L-bands for multi-frequency analysis for tropical forest AGB and C estimation. The study revealed information regarding the spatial distribution and quantification of forest AGB and C required for REDD monitoring.

## 1. INTRODUCTION

'400 ppm World'; an universal alarming situation where the global carbon dioxide ($CO_2$) concentration surpassed the 400 ppm threshold level during 2016; a phenomenon which is permanent not likely to revert back in future (Betts et al., 2016). India being a mega-biodiversity country harbors forests that account for more than one fifth of the geographical area. Indian tropical forests are likely to experience extreme hasty and significant climate and vegetation changes over the next decades (Ravindranath et al., 2006). Globally this is a serious issue as tropical forests sequester one fifth of the global carbon (C) stock, and almost one half of the above-ground C, stored in vegetation of all biomes (Hunter et al., 2013). Biophysical indicators of forest C storage, viz. the above-ground biomass (AGB) are important for realizing the terrestrial C equilibrium (Sinha et al., in press). Sequestration of C in the vegetation is the only possible viable strategy in milieu of Reducing Emissions from Deforestation and forest Degradation (REDD) to maintain the atmospheric C balance and account for the $CO_2$ released from forests (Waikhom et al., 2017). Henceforth, accurate estimates of biomass are a prerequisite for forest C accounting under REDD framework (Sinha et al., 2016).

Sinha et al. (2015) have outlined detailed information regarding the biomass estimation methods, wherein, the remote sensing (RS)-based approaches have clearly outshined other methods. Optical sensors are recurrently used

for AGB estimation (Kumar et al., 2013; Sharma et al., 2013), however, saturates early owing to poor sensitivity to forest parameters, unlike Synthetic Aperture Radar (SAR) and Light Detecting and Ranging (LiDAR) sensors (Sinha et al., 2015). Though both the systems are sensitive to forest spatial structure and standing biomass, SAR is favoured due to its wall-to-wall coverage which is absent in all LiDAR systems (Su et al., 2016). Currently SAR is extensively used in retrieving forest biomass (Sinha et al., 2015).

Usually SAR data are acquired in X, C, L bands and sometimes in S and P bands as well. SAR backscatter from longer wavelengths, like L- and P-bands relate more to the forest biophysical parameters due to their greater penetration capabilities through the vegetation surfaces and are scattered/attenuated by trunk and main branches (Sinha et al., 2015). Synergic use of radar and optical sensor data has the potential to improve the estimation of forest AGB (Sinha et al., 2016). However, optical sensors suffers several drawbacks, like occurrence of frequent clouds in the tropics hampering the acquisition of the high quality satellite data, lack of volumetric estimations due to absence of penetrability of visible bands and low saturation levels of the spectral bands for biomass estimation (Sinha et al., 2015). Hence, the use of integrated multi-frequency SAR reveals greater potential for AGB estimation that can possibly overcome the limitations of optical sensors and single SAR sensors. Alappat et al. (2011) applied synergic model integrating SAR C- and L-bands and Englhart et al. (2011) used SAR X- and L-bands for biomass assessment. This study in addition integrates SAR backscatter data from X-, C- and L-bands to investigate relationships with field AGB to derive a synergic model to estimate above-ground bole biomass, from which C and $CO_2$ has been enumerated.

## 2. MATERIALS AND METHODS

### 2.1 Site under investigation

Munger forests in the state of Bihar (India) comprising the Bhimbandh Wildlife Sanctuary with geographic coordinates of 25º19'30"N-24º56'50"N latitude and 86º33'33"E-86º11'51"E longitude, covering an area of approx 672.5 $km^2$ has been considered as the test site for investigation (Figure 1). Summer temperature reaches 45$^oC$, while winter experiences nearly 3-9$^oC$. The average annual rainfall is around 1079 mm.

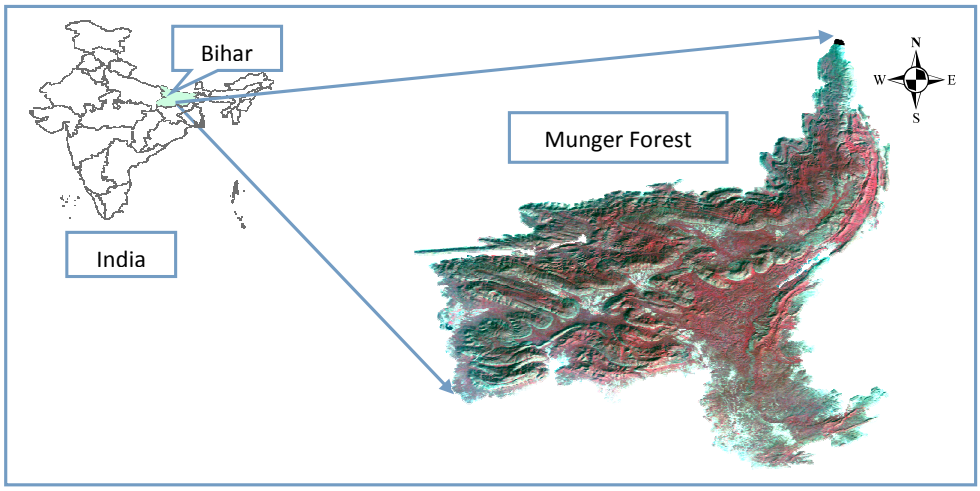


Figure 1: Location of the study site

### 2.2 Land use land cover details

The backdrop of the site is a moist-deciduous mixed forest with over 89% of the area under forests. The study site mainly comprises of open and degraded mixed forests, with *Shorea robusta*, *Acacia catechu*, *Madhuca longifolia*, *Dendrocalamus strictus*, *Diospyros melanoxylon* and *Terminalia tomentosa* as the dominant floral species (Sinha et al., 2013). Located south of River Ganges, the entire area is drained by several small rivers, like Kiul, Man, Narokol, Morwe, Dudhpanian, Kandani, etc. The forest is a virgin patch with limited disturbances in terms of deforestation mainly due to dispersed anthropogenic activities like settlements, agricultural development and plantations and to some extent mining activities. Conservation of the forest is of high relevance for the conservation of biodiversity and also in context to REDD/REDD+.

### 2.3 Data input

Multi-frequency SAR datasets of COSMO-Skymed, Radarsat-2 and ALOS PALSAR were procured to model for AGB prediction. The COSMO-Skymed data is HH/VV dual polarized X-band obtained through PINGPONG imaging mode with 15m (resampled to 25m) spatial resolution and 30km swath width. The Radarsat-2 data is Standard Quad-pol C-band with 25m spatial resolution and 25km swath width. The ALOS PALSAR data is L-band acquired in Fine Beam Single (HH) and Dual (HH,HV), and Quad Polarimetric (HH,HV,VH,VV) mode with 25m spatial resolution, and off-nadir angles of 34.3° and 21.5°, and swath width of 70 and 30 km respectively. Simultaneously, primary data was generated in terms of field inventory that included in-situ information generated from field sample plots, like forest types, canopy density, species composition, stand height, and girth at breast height (GBH).

### 2.4 In-situ field inventory for field biomass estimation

A total of 45 square sample plots of 0.1 ha (Hectare) were randomly selected, 36 of which were considered for developing models, while the remaining for validating the models. The three most important data collected from field within each plot i.e., tree species, stand height and GBH; from which the diameter at breast height (DBH) were used to calculate the volume using the species-specific regional volumetric equations of FSI (1996). AGB is then estimated by multiplying the resulting volume with the tree-specific specific gravity of FRI (1996). Global Positioning System (GPS) was used to collect the latitude-longitude information of the plots for importing the information in GIS framework. Volumetric equations and specific gravity of the tree species for the study site are mentioned in Sinha (2016).

### 2.5 SAR processing

Raw SAR datasets were preprocessed, rectified, geocoded and calibrated using a series of standard steps in SARscape software to generate the backscatter image following the equation (Sinha et al., 2016):

$$\sigma^0 = 10 \times a \log 10(DN) + A_0 \quad (1)$$

where, $\sigma^0$ = backscatter coefficient or sigma nought values in decibels (dB),DN is the power (or intensity) image, $A_0$ is the calibration factor that vary with sensor type. $A_0$ = -115 dB for ALOS PALSAR, $A_0$ = -59.62 dB for HH polarized COSMO-Skymed, $A_0$ = -58.88 dB for VV polarized COSMO-Skymed. Radarsat-2 has different values of $A_0$ for each line and is processed in Geomatica.

### 2.6 Model development

SAR backscatter values were regressed to the 36 field-based AGB values to find the best fit model for calculating AGB. The field-based estimated AGB was correlated with modeled AGB for 9 additional random points for validation of the best-fit model. The model performance was evaluated based on certain statistical measures (Sinha et al., 2016). Resulting modeled AGB (in t/ha) were converted to carbon (C) and carbon dioxide ($CO_2$) equivalents using conversion factors of 0.5 and 3.67 respectively (Mushtaq & Malik, 2014, Rashid et al., 2016).

## 3. RESULTS

### 3.1 SAR interactions with AGB

X-, C- and L-bands were used to develop the AGB model. Figure 2 shows the relationship between the SAR backscatter values and the in-situ plot AGB values, which showed the existence of a logarithmic relation. The figure also revealed that X-band saturated earliest, then the C-band, and lastly the L-band. The saturation level depended on the radar frequency or wavelength, radar wave polarization and vegetation types.

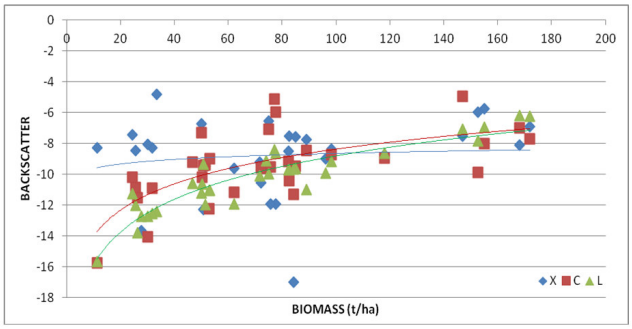


Figure 2: Relationship between multi-frequency SAR backscatter with plot AGB

X-band COSMO-Skymed VV polarized data interacted with the upper part of the canopy (leaves, small branches, etc.); as revealed by the increased $r^2$ value in comparison to HH. With minimum penetration capability, X-band has the minimum interaction with the trunk and the main branches, so has the poorest relationship with the bole AGB. C-band having relatively greater penetration within the canopy layer interacts with the secondary branches and this is evident from higher $r^2$ values. L-band ALOS PALSAR showed the best correlation with the bole AGB due to its ability to penetrate the canopy layer and interact with the trunk. HH polarized data of L-band showed the greatest interaction with the trunk due to its vertical structure. Hence, HH polarization was most sensitive towards the bole AGB. It was observed that like-polarizations had high backscatter values than cross-polarizations and increase in the wavelength leads to increase in the penetration capability of the radar signals, thus providing more accurate information related to the bole above-ground biomass. Table 1 documents the correlation values. In this study, X-band saturates earlier at about 40-50 t/ha, while C-band saturates next nearly at 100-120 t/ha, while, saturation is highest for L-band among the three, at about 160-180 t/ha (Figure 2).

Table 1: Coefficient of determination ($r^2$) between SAR backscatter and plot AGB

| SAR datasets | Polarization | $r^2$ |
|---|---|---|
| X-band COSMO-Skymed | HH | 0.01 |
| X-band COSMO-Skymed | VV | 0.02 |
| C-band Radarsat-2 | HH | 0.46 |
| C-band Radarsat-2 | HV | 0.34 |
| C-band Radarsat-2 | VV | 0.43 |
| L-band ALOS PALSAR | HH | 0.85 |
| L-band ALOS PALSAR | HV | 0.56 |

### 3.2 Integrated AGB model

Three best-fit models (Equations 2, 3 and 4) were generated from this logarithmic relationship between backscatter values from each of the three SAR datasets (X-, C- and L-band respectively) and the plot AGB based on the information in Table 1 from 36 plots used for model development and calibration. Synergic modeling was developed using only those plots among the total 36 that were found in all the SAR datasets. An integrated AGB model was developed using Multiple Linear Regression (MLR) of Equations 2, 3 and 4 where the data were used in combination of all three datasets, expressed as Equation 5. The models are enlisted in Table 2. The models were evaluated based on certain statistical calculation, also documented in Table 2. The table indicated that the synergic model integrating SAR X-, C- and L-bands (Equation 5) showed the best results among all; while Equation 4 involving just the L-band showed better results among all the single band models.

Table 2: AGB model evaluation

| Eq. | Model | SAR data used | $r^2$ | RMSE (t/ha) |
|---|---|---|---|---|
| 2 | $94.984 * e^{\left(0.0442 * \sigma^o_{X\_VV}\right)}$ | X (VV) | 0.01 | 46.18 |
| 3 | $380.58 * e^{\left(0.1874 * \sigma^o_{C\_HH}\right)}$ | C (HH) | 0.28 | 37.24 |
| 4 | $1067.3 * e^{\left(0.2765 * \sigma^o_{L\_HH}\right)}$ | L (HH) | 0.87 | 16.06 |
| 5 | $103.504 * e^{\left(0.0442 * \sigma^o_{X\_VV}\right)} - 44.3375 * e^{\left(0.1874 * \sigma^o_{C\_HH}\right)} + 1028.984 * e^{\left(0.2765 * \sigma^o_{L\_HH}\right)} - 58.8778$ | L (HH), C (HH), X (VV) | 0.90 | 15.29 |

### 3.3 Validation

The AGB models were statistically validated with nine additional plot AGB data and the corresponding statistical measures, like $r^2$, RMSE, slope, average absolute accuracy ($\varsigma$) and Willmott's Index of agreement ($d$) were executed. The results are summarized in Table 3. The table confirmed that the integrated AGB model (Equation 5) showed the best results with the highest $r^2$ value of 0.954, least RMSE of 14.813 t/ha, good model accuracy of about 79% and greatest $d$ value of 0.95. Significantly high $r^2$, model accuracy and $d$ values nearing unity and low RMSE value reveal the acceptability of the model. However, Equation 4 with L-band information also showed promising results amongst the single sensor models with a fairly high $r^2$ value of 0.713, moderate RMSE of 22.34 t/ha, good model accuracy of 61.7% and $d$ value of 0.88.

Table 3: AGB model validation

| Eq. | $r^2$ | RMSE (t/ha) | Slope | ς | *d* |
|---|---|---|---|---|---|
| 2 | 0.094 | 32.151 | 0.105 | 39.478 | 0.306 |
| 3 | 0.002 | 50.083 | -0.050 | 7.961 | -0.095 |
| 4 | 0.713 | 22.340 | 0.871 | 61.768 | 0.883 |
| 5 | 0.954 | 14.813 | 0.964 | 78.894 | 0.950 |

### 3.4 AGB and C maps

The AGB map represented as Figure 3 was prepared from Equation 5 in GIS and reclassified in ten classes according to biomass levels from very low (<25t/ha and 25-50 t/ha), low (50-75t/ha and 75-100t/ha), moderate (100-125t/ha and 125-150t/ha), high (150-175t/ha and 175-200t/ha) to very high (>250t/ha). Resulting modeled AGB were converted to carbon (C) and carbon dioxide ($CO_2$) equivalents using conversion factors and reclassified in five classes. Figure 4 illustrates both C and $CO_2$ spatial distribution map. Both the figures 3 and 4 have white or empty regions within the boundary of the study area that lack the input SAR data owing to data restrictions. North portion of the of study site in the figures show erroneous results due to presence of non-overlapping portions of multi-sensor satellite data, demarcated in blue dotted line.

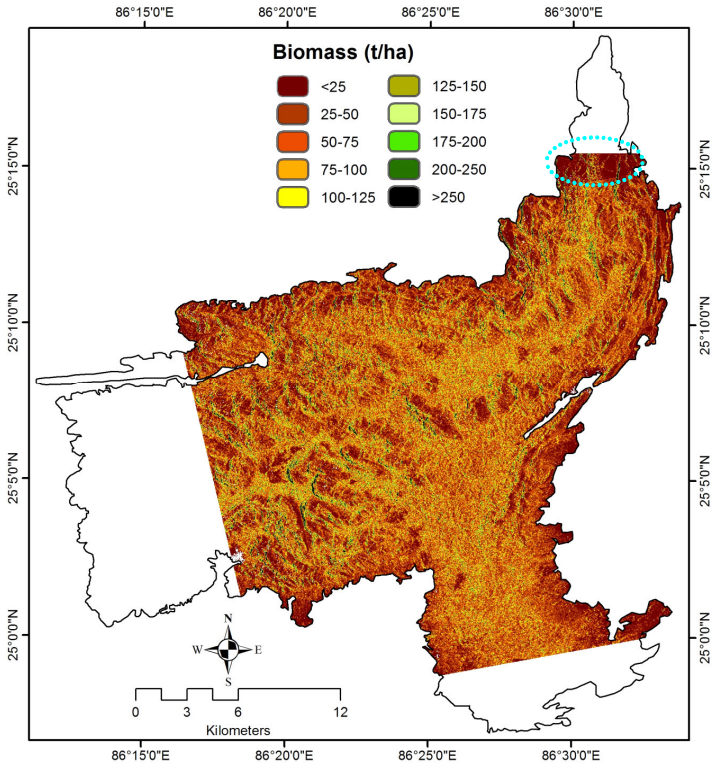


Figure 3: AGB map developed from integrated model

Figure 3 portrays less vegetative parts with low biomass levels of <50 t/ha at the vicinity of the boundary of the study area, water bodies and the built-up regions that are concentrated in the periphery and at the central parts. Most of the forested region was observed to lie within the biomass range of 25–100 t/ha, with an average value of 56.24 t/ha. Most of the high density vegetation was observed to have biomass ranging from 75–125 t/ha, mostly covering the interior parts of the study area; however, some scattered areas with even higher biomass values that too are generally restricted to the interior regions. Likewise, Figure 4 shows similar observation as C and $CO_2$ were observed to be concentrated more in the interior parts of the area. Average C was calculated to 28.12 t/ha, while $CO_2$ was 103.2 t/ha. It can be also noticed that the relative early saturation of biomass with the use of single SAR frequency data alone can be counteracted with the integrated use of multi-frequency SAR data due to the better relationship of AGB compartments to each of the SAR frequency bands. Hence, the integrated multi-frequency SAR model provided the most accurate result for predicting AGB.

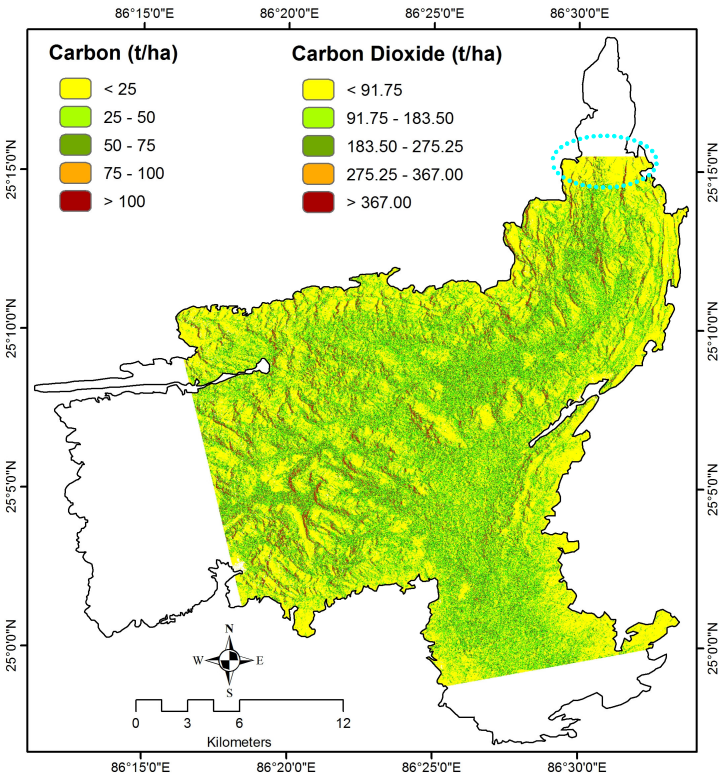


Figure 4: C and $CO_2$ spatial map

## 4. CONCLUSIONS

In this '400 ppm World', global climate change is the most alarming situation that this world is experiencing. In this context, REDD and associated concepts are gaining attention; henceforth, biomass/carbon assessment is becoming crucial to address this issue. The current study targets in using multi-frequency SAR to assess above-ground bole biomass and in-turn the forest carbon stock over a tropical deciduous heterogeneous virgin forest patch of Munger in India. Synergic use of multi-frequency SAR has the potential to augment the AGB estimations in comparison to any optical data as well as any single frequency spaceborne SAR data till date. Out of the X-, C- and L-bands, the best model predicting AGB comprises of L-band information. Subsequently, the estimation improves on integrating all the three SAR wavelength bands. The exponential model was observed as the best fit model for estimating biomass on regressing SAR backscatter values to plot estimated AGB. The integrated model was validated and $r^2$ of 0.95, RMSE of 14.81 t/ha, model accuracy of 79% and Willmott's index of agreement of 0.95 was calculated without much over or under-estimation as denoted by the slope value of 0.96. The consequence of the approach in resolving the relative early saturation of biomass with optical RS data or single SAR frequency data alone is evident thus can be counteracted with the integrated use of multi-frequency SAR data due to the better relationship of AGB compartments.

Hence, in this study, a synergy regression model for predicting AGB was developed with synergic use of SAR multi-frequency X-, C- and L-band information that was further transformed to generate C stock and $CO_2$ emission models in GIS. Quantifying multi-temporal changes in $CO_2$ via this approach can account for the climate change. The integrated multi-frequency SAR approach adopted in the study gave valuable information of the spatial distribution and quantification of the forest biomass and carbon; important for REDD monitoring.

## 5. ACKNOWLEDGEMENTS

The authors sincerely acknowledge Space Application Centre (ISRO, India) for providing technical help and JAXA (Japan), CSA (Canada) and ASI (Italy) for providing SAR data through ALOS-RA Cosmo Skymed A.O. project. The first author expresses sincere gratitude to Science and Engineering Research Board (SERB), Department of Science and Technology (DST), Government of India for providing funds under SERB National Post-Doctoral fellowship (SERB NPDF) scheme (File Number: PDF/2015/000043).

## 6. REFERENCES


Alappat, V. O., Joshi, A. K. and Krishnamurthy, Y. V. N., 2011. Tropical dry deciduous forest stand variable estimation using SAR data. Journal of the Indian Society of Remote Sensing, 39 (4), pp. 583-589.

Betts, R. A., Jones, C. D., Knight, J. R., Keeling, R. F. and Kennedy, J. J., 2016. El Niño and a record $CO_2$ rise. Nature Climate Change, 6, pp. 806–810.

Englhart, S., Keuck, V. and Siegert, F., 2011. Aboveground biomass retrieval in tropical forests — the potential of combined X- and L-band SAR data use. Remote Sensing of Environment, 115, pp. 1260-1271.

FRI, 1996. Indian Woods. Forest Research Institute, Dehradun.

FSI, 1996. Volume equations for forests of India, Nepal and Bhutan. Forest Survey of India, Ministry of Environment and Forests, Government of India, Dehradun.

Hunter, M. O., Keller, M., Victoria, D. and Morton, D. C., 2013. Tree height and tropical forest biomass estimation. Biogeosciences, 10, pp. 8385–8399.

Kumar, P., Sharma, L. K., Pandey, P. C., Sinha, S. and Nathawat, M. S., 2013. Geospatial strategy for tropical forest-wildlife reserve biomass estimation. IEEE Journal of Selected Topics in Applied Earth Observations and Remote Sensing, 6 (2), pp. 917–923.

Mushtaq, H. and Malik, T., 2014. Accounting carbon dioxide emission and stratification of carbon stock in Western Ghats, India. A geospatial approach. International Journal of Remote Sensing & Geoscience, 3 (1), pp. 1-5.

Rashid, I., Bhat, M. A. and Romshoo, S. A., 2016. Assessing changes in the above ground biomass and carbon stocks of Lidder valley, Kashmir Himalaya, India. Geocarto International, doi: 10.1080/10106049.2016.1188164.

Ravindranath, N. H., Joshi, N. V., Sukumar, R. and Saxena, A., 2006. Impact of climate change on forests in India. Current Science, 90 (3), pp. 354–361.

Sharma, L. K., Nathawat, M. S. and Sinha, S., 2013. Top-down and bottom-up inventory approach for above ground forest biomass and carbon monitoring in REDD framework using multi-resolution satellite data. Environmental Monitoring and Assessment, 185 (10), pp. 8621–8637.

Sinha, S., 2016. Polarimetric Scattering Parameter products of ALOS PALSAR for forest biomass assessment. Research & Reviews: Journal of Space Science & Technology, 5 (1), pp. 1-9.

Sinha, S., Jeganathan, C., Sharma, L. K. and Nathawat, M. S., 2015. A review of radar remote sensing for biomass estimation. International Journal of Environmental Science and Technology, 12 (5), pp. 1779-1792.

Sinha, S., Jeganathan, C., Sharma, L. K., Nathawat, M.S., Das, A.K. and Mohan, S., 2016. Developing synergy regression models with space-borne ALOS PALSAR and Landsat TM sensors for retrieving tropical forest biomass. Journal of Earth System Science, 125 (4), pp. 725-735.

Sinha, S., Santra, A., Sharma, L. K., Jeganathan, C., Nathawat, M.S., Das, A.K. and Mohan, S., in press. Forest vigor assessment in terms of above ground biomass using multi-polarized Radarsat-2 satellite sensor. Journal of Forestry Research.

Sinha, S., Sharma, L. K. and Nathawat, M. S., 2013. Integrated geospatial techniques for land-use/land-cover and forest mapping of deciduous Munger forests (India). Universal Journal of Environmental Research and Technology, 3 (2), pp. 190-198.

Su, Y., Guo, Q., Xue, B., Hu, T., Alvarez, O., Tao, S. and Fang, J., 2016. Spatial distribution of forest aboveground biomass in China: Estimation through combination of spaceborne lidar, optical imagery, and forest inventory data. Remote Sensing of Environment, 173, pp. 187–199.

Waikhom, A. C., Nath, A. J. and Yadava, P. S., 2017. Aboveground biomass and carbon stock in the largest sacred grove of Manipur, Northeast India. Journal of Forestry Research, doi: 10.1007/s11676-017-0439-y.